

Dust Extinction in Star-forming Galaxies from near-IR Spectroscopy

Domínguez et al. 2013, ApJ, 763, 145

Alberto Domínguez

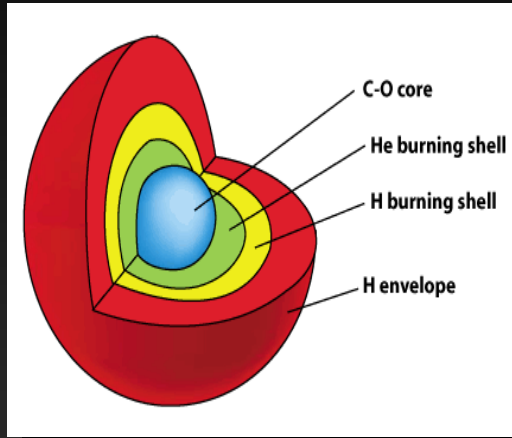
(Grupo de Altas Energías,
Universidad Complutense de Madrid)

in collaboration with Brian Siana (UC Riverside)
& the WISP team

ESAC, Madrid,
April 23-25, 2018

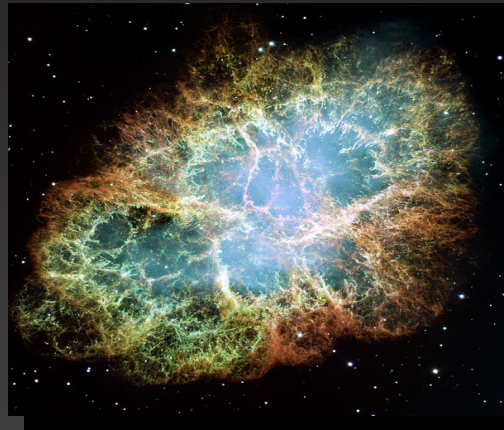
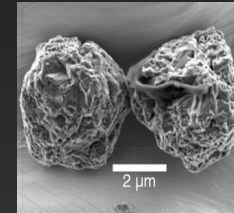
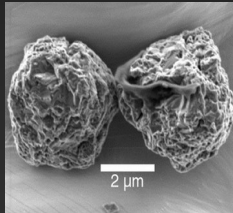
What is and where is dust produced?

Asymptotic-giant-branch stars



ISM

ISM



Supernovae

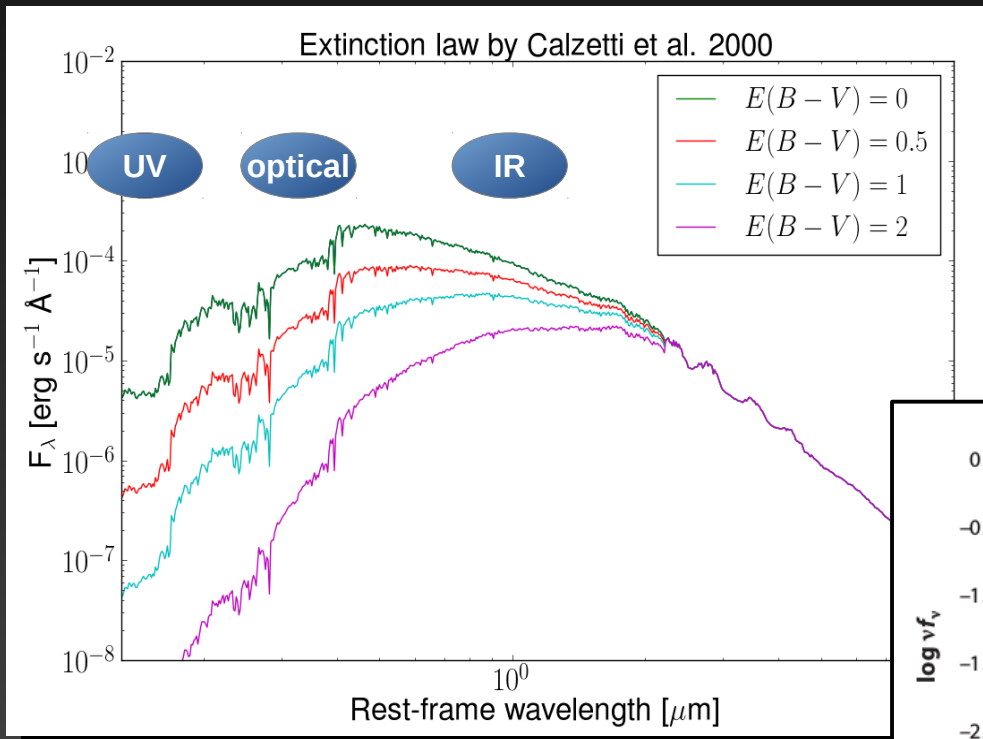
ISM

ISM

Effects of the interstellar dust

Dimming

Reddening



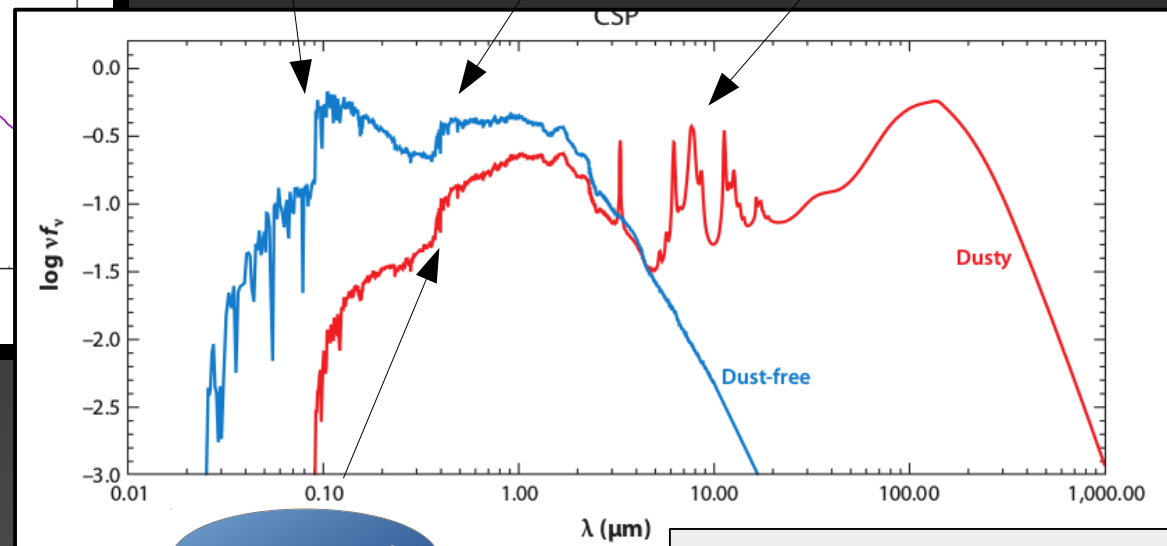
Color index

$$E_{B-V} = (B - V)_{\text{observed}} - (B - V)_{\text{intrinsic}}$$

Ly break, 912 Å

Ba break, 3646 Å

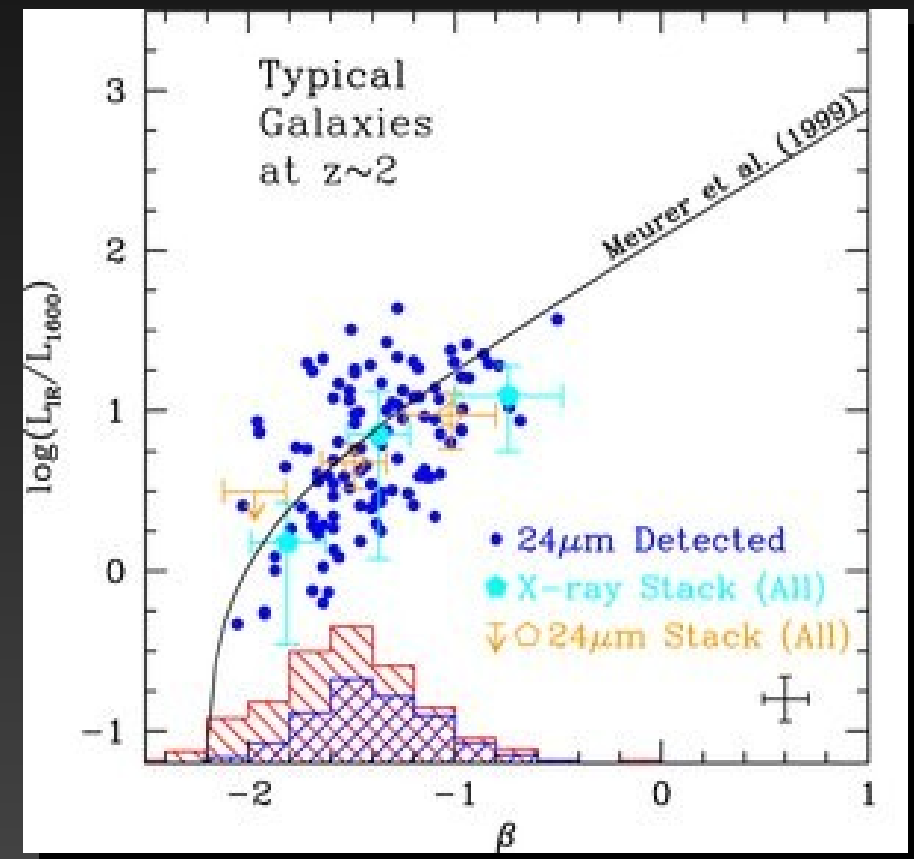
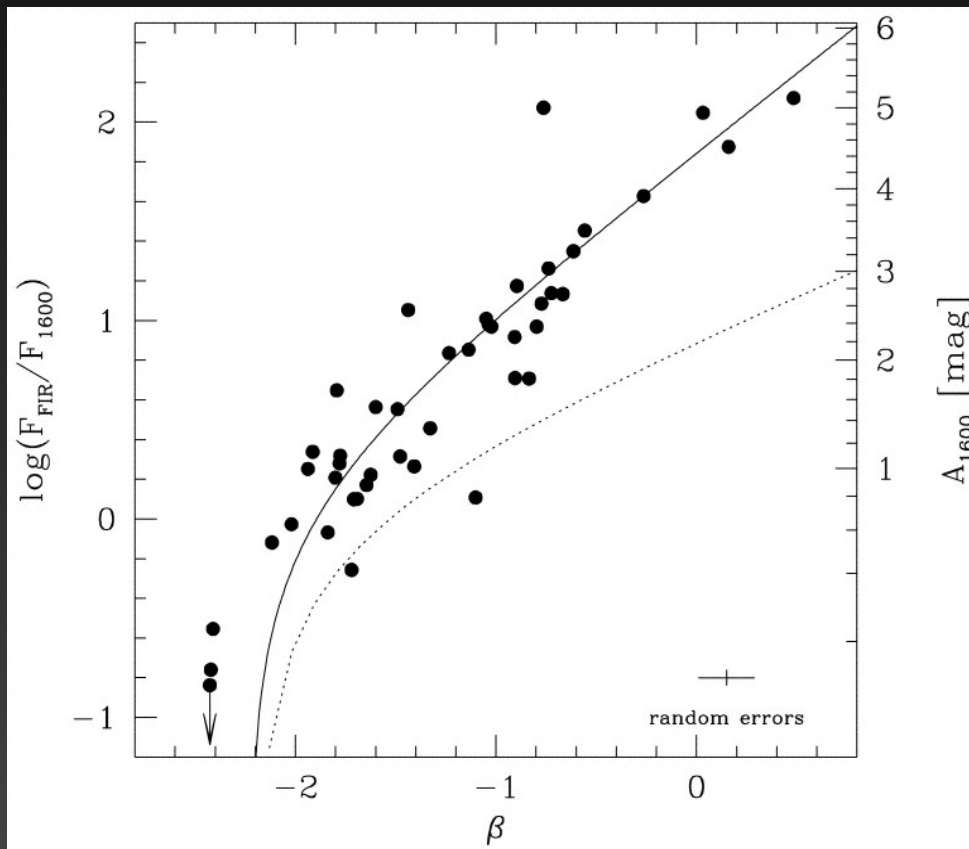
PAH



Conroy 2013

Methodologies for studying dust extinction

UV slopes and infrared observations that probes stellar-continuum extinction (e. g. Meurer et al. 1999; Reddy et al. 2010; Bouwens et al. 2011)



$$f_{\lambda} \propto \lambda^{\beta} \quad (\text{from } \sim 1300 \text{ \AA} \text{ to } 3500 \text{ \AA})$$

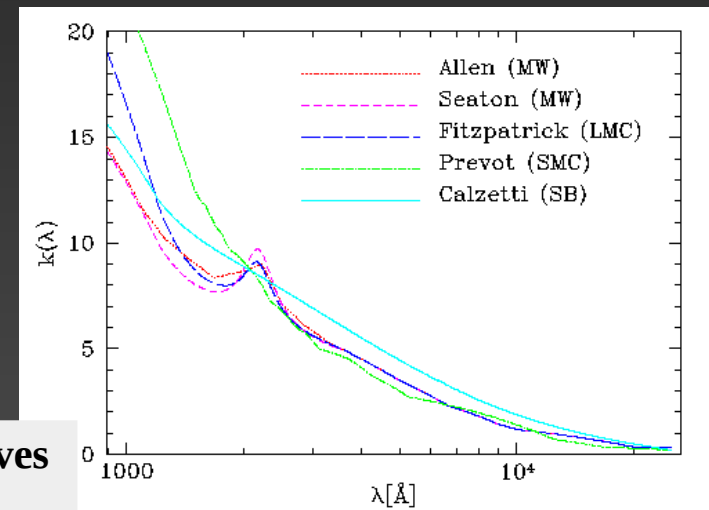
Methodologies for studying dust extinction

Emission-line ratios such as Balmer emission lines that probes HII-regions extinction (e. g. Kennicutt et al. 1992; Hopkins et al. 2001; Brinchmann et al. 2004; Garn & Best 2010).

Transition of n	3 → 2	4 → 2	5 → 2	6 → 2
Name	H α	H β	H δ	H γ
Wavelength (\AA)	6563	4861	4341	4102

Balmer series

$$E(B - V) = \frac{2.5}{k(\lambda_{H\beta}) - k(\lambda_{H\alpha})} \log_{10} \left[\frac{(H\alpha/H\beta)_{obs}}{(H\alpha/H\beta)_{int}} \right]$$



The Balmer decrement of Sloan Digital Sky Survey galaxies

Brent Groves,^{1,2*} Jarle Brinchmann¹ and Carl Jakob Walcher³

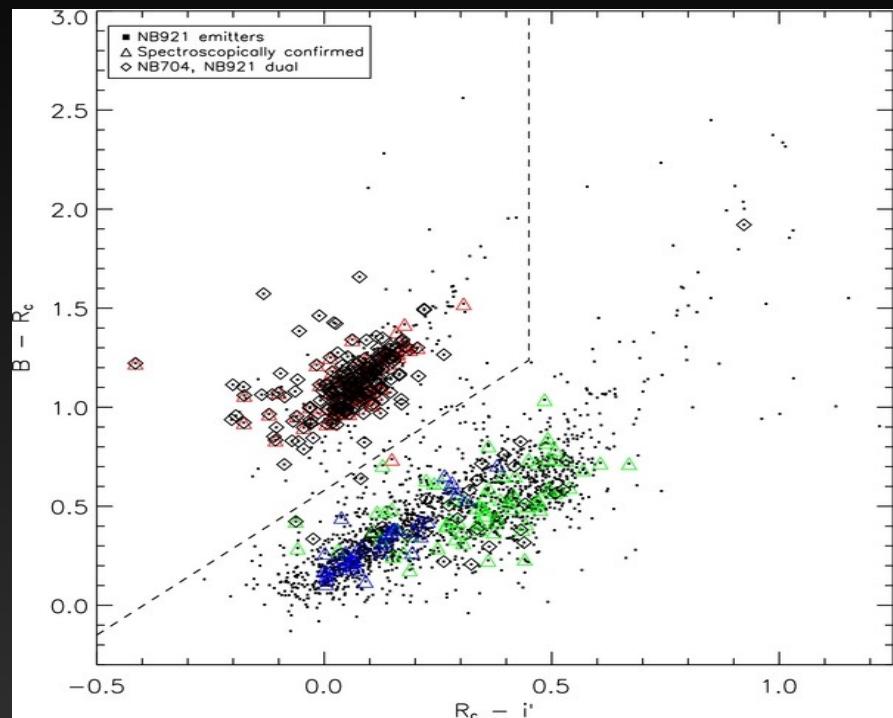
¹Leiden Observatory, Leiden University, PO Box 9513, 2300 RA Leiden, the Netherlands

²Max Planck Institute for Astronomy, Königstuhl 17, D-69117 Heidelberg, Germany

³Astrophysikalisches Institut Potsdam, An der Sternwarte 16, D-14482 Potsdam, Germany

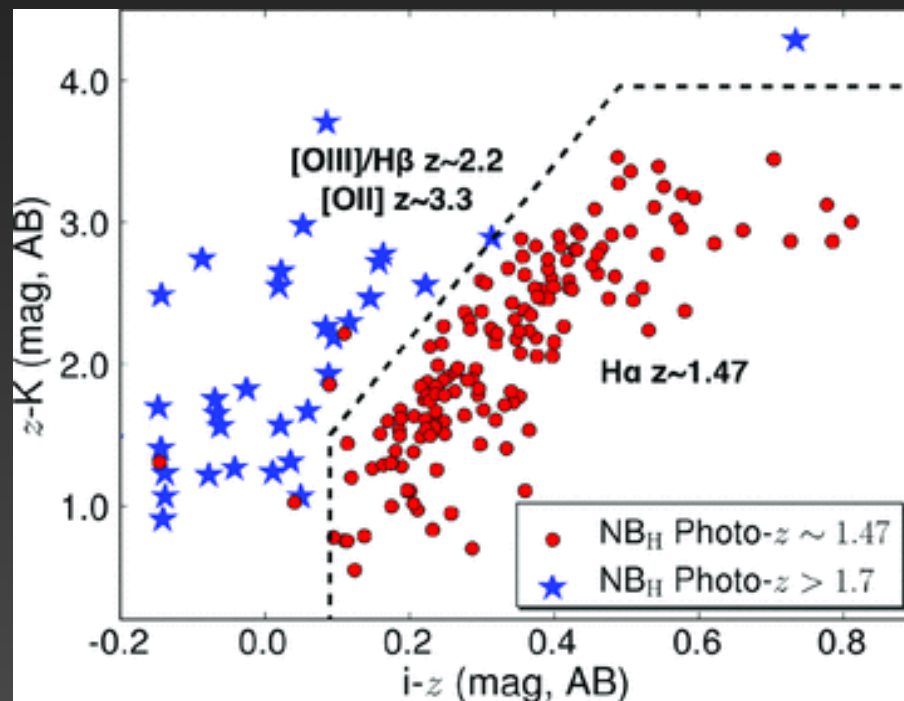
**Empirical extinction curves
from Hyperz manual**

Dust extinction at $z > 0.5$ from emission-line ratios



Ly et al. 2012 at $z \sim 0.5$ →
combination of photometry
and spectroscopy

Sobral et al. 2012 at $z \sim 1.5$
→ $H\alpha/[O II]$ with $[O II]$
being significantly
dependent on metallicity.



The WFC3 Infrared Spectroscopic Parallel (WISP) survey

- Pure parallel Hubble Space Telescope program (PI Matthew Malkan, UCLA) with more than 1500 orbits, approximately 390 high-latitude fields observed so far.
- The faintest galaxies are 3 times fainter than galaxies previously studied at $z \sim 1.5$.

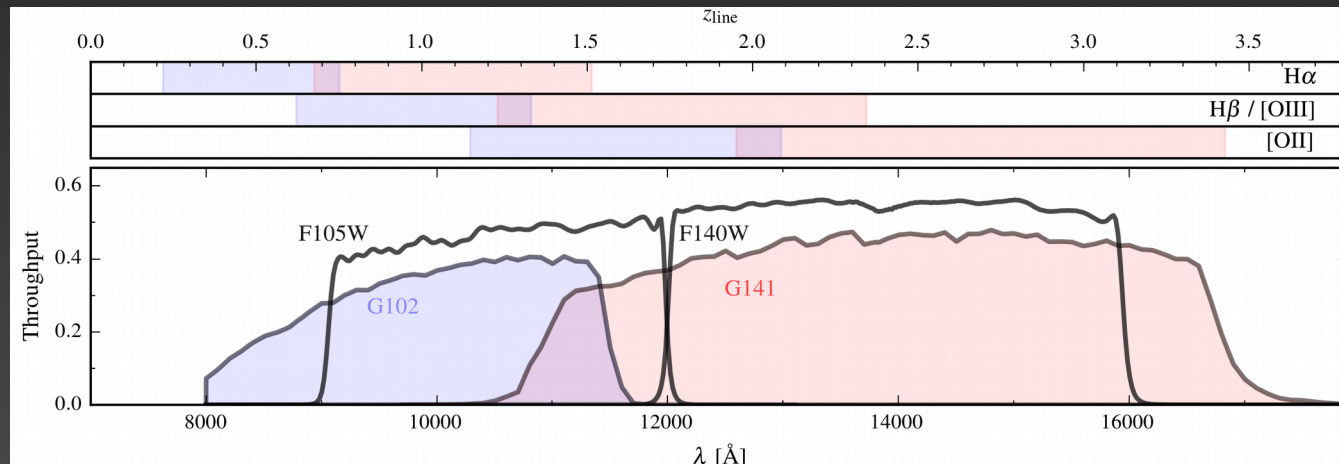
GRISMS near-IR spectroscopy

G102: $0.80 \leq \lambda \leq 1.17 \mu\text{m}$ ($R \sim 210$)

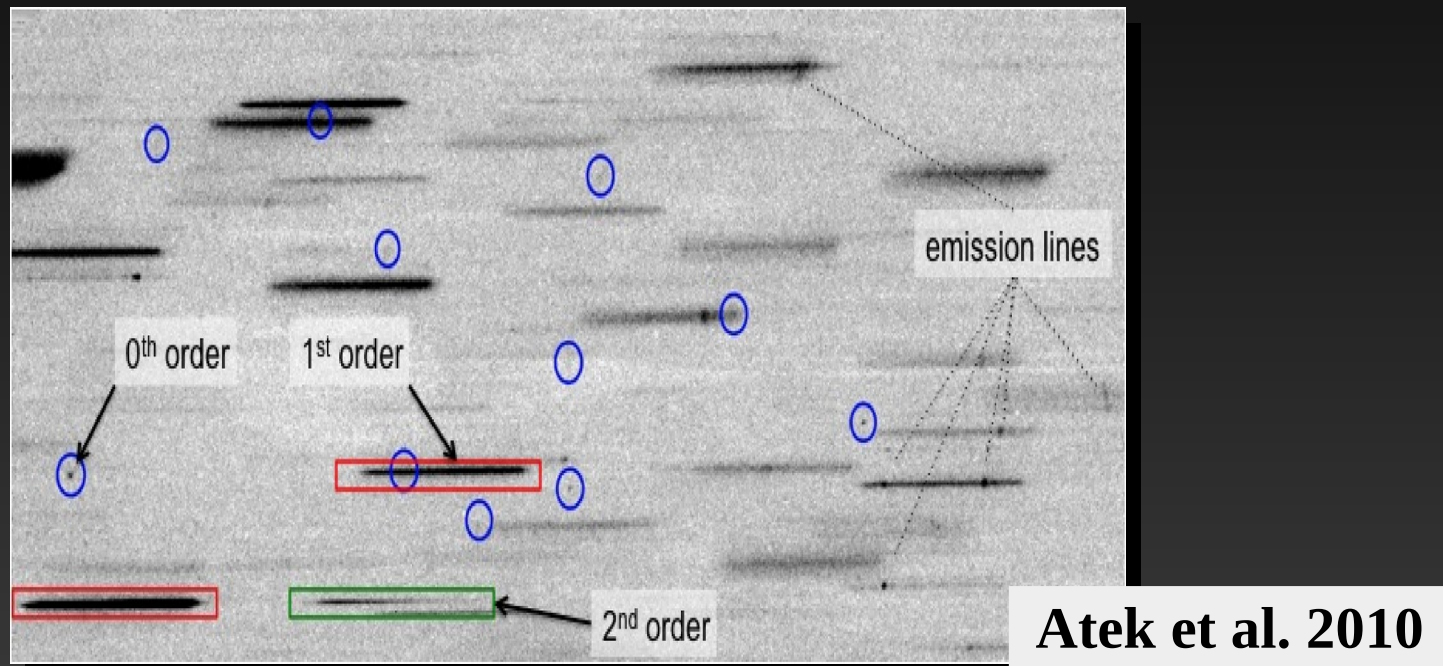
G141: $1.11 \leq \lambda \leq 1.67 \mu\text{m}$ ($R \sim 130$)

Direct-imaging photometry:

F475X, F600LP, F110W, F160W
and **IRAC 3.6 μm**



The WFC3 Infrared Spectroscopic Parallel (WISP) survey

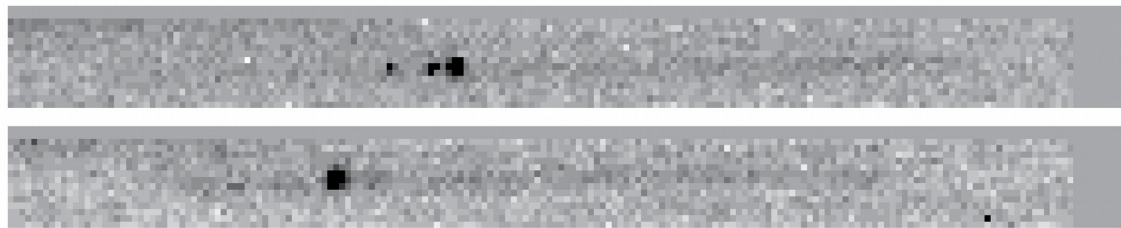
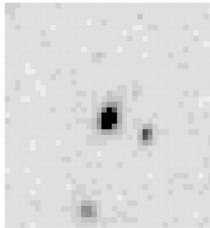


Example of different spectral features in one G141 grism image.

Field of view IR Channel: 123 x 136 arcsec

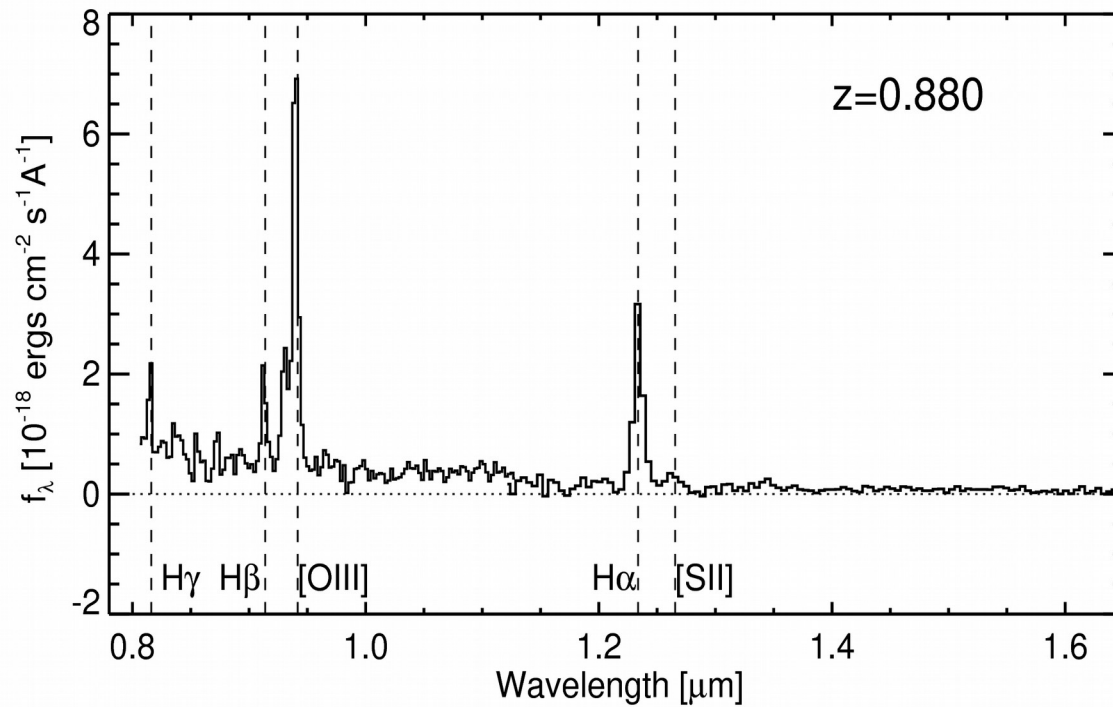
The WISP survey

F110W



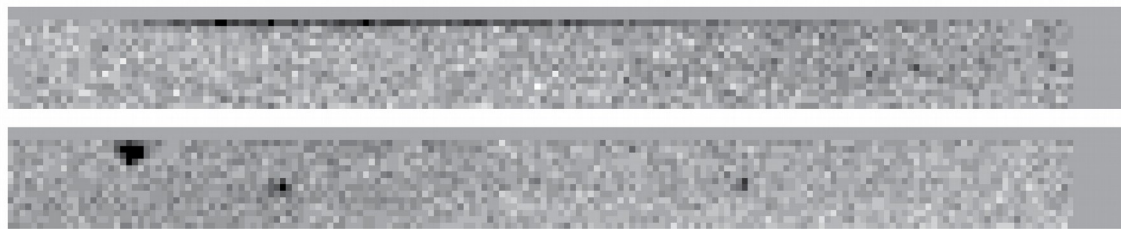
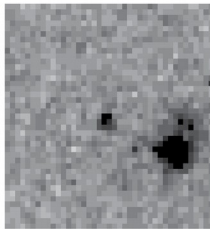
G102

G141



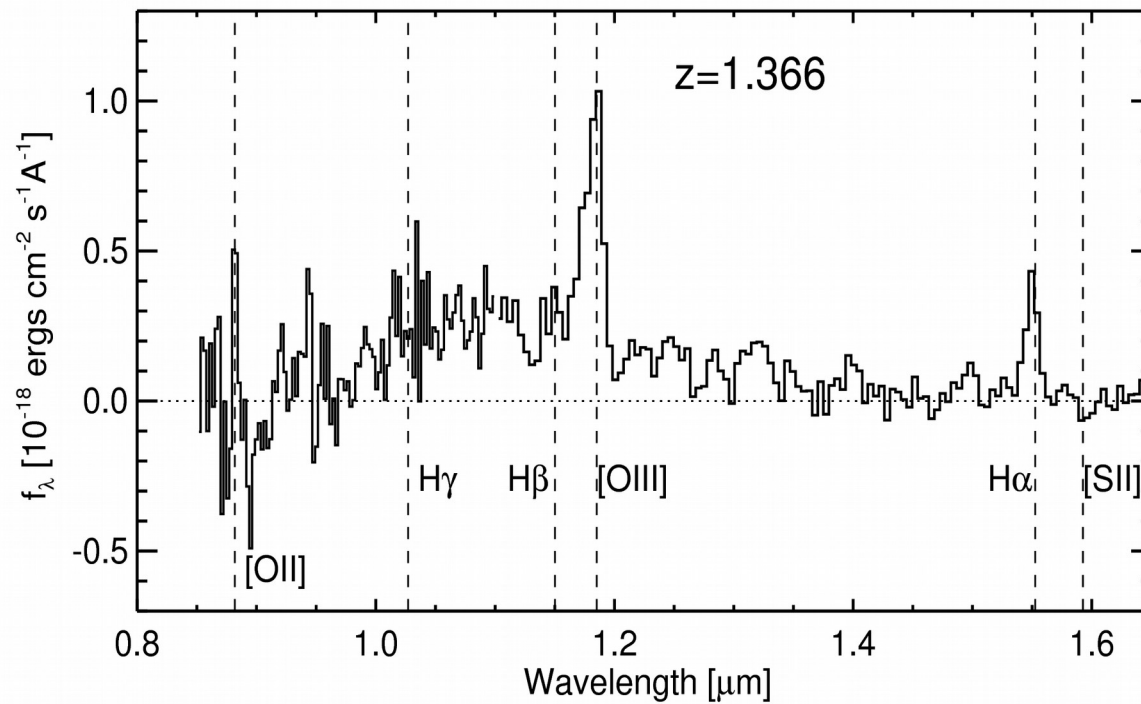
The WISP survey

F110W

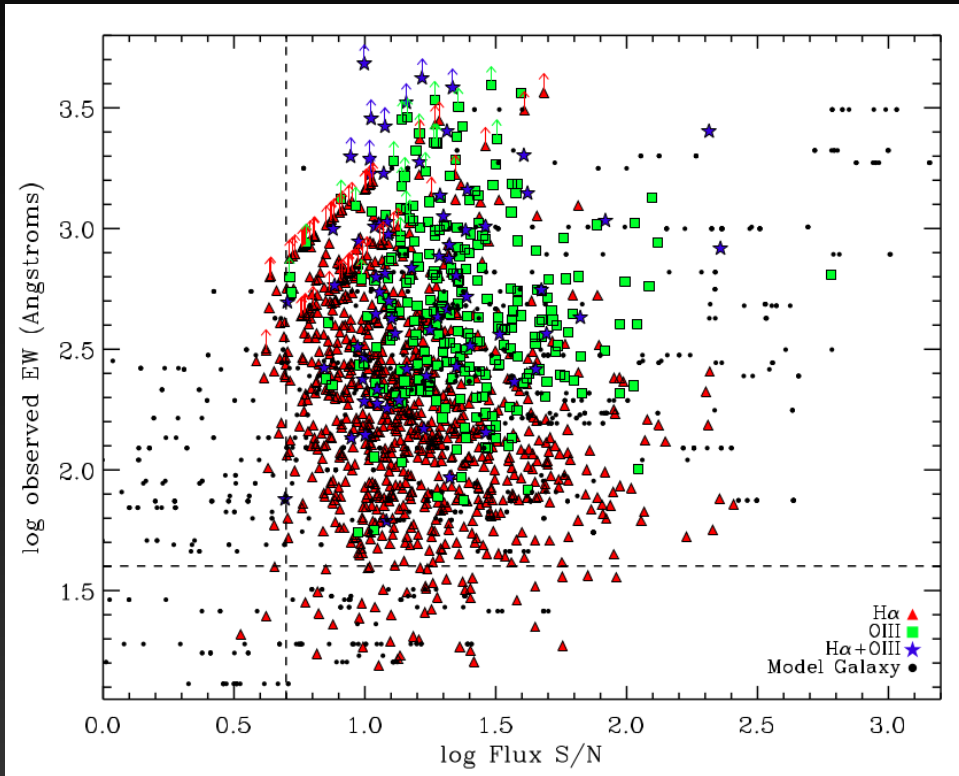


G102

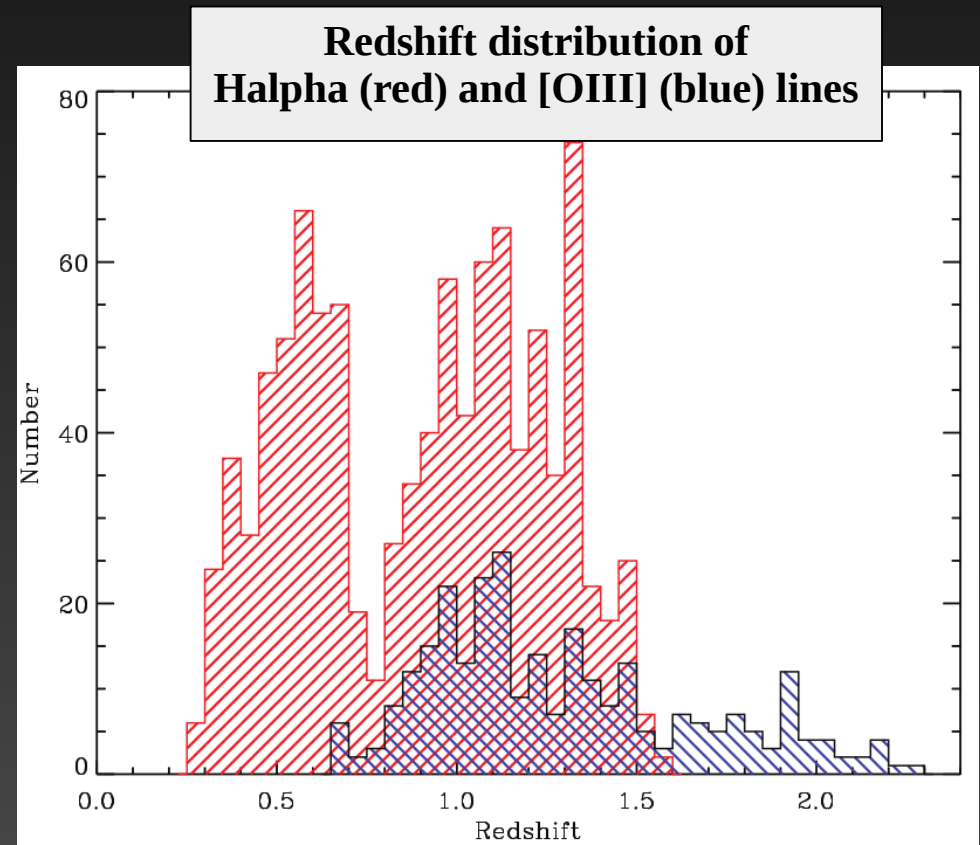
G141



General properties of WISP galaxies



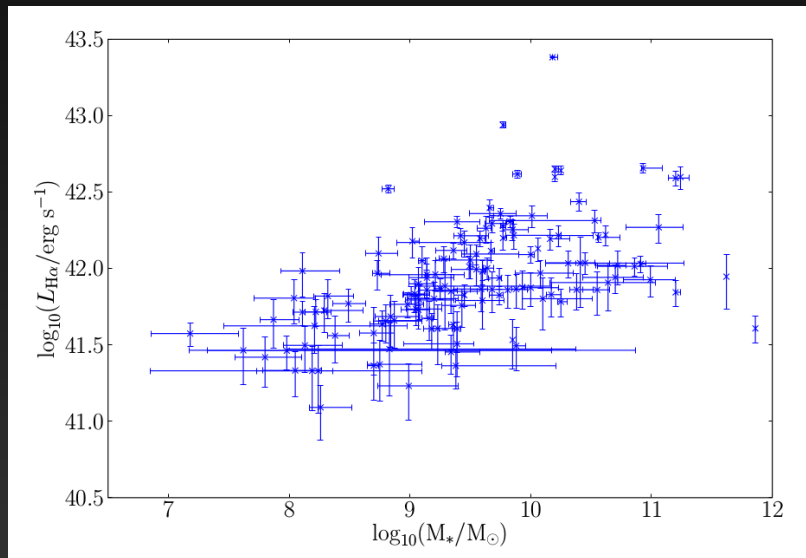
EW versus flux signal/noise



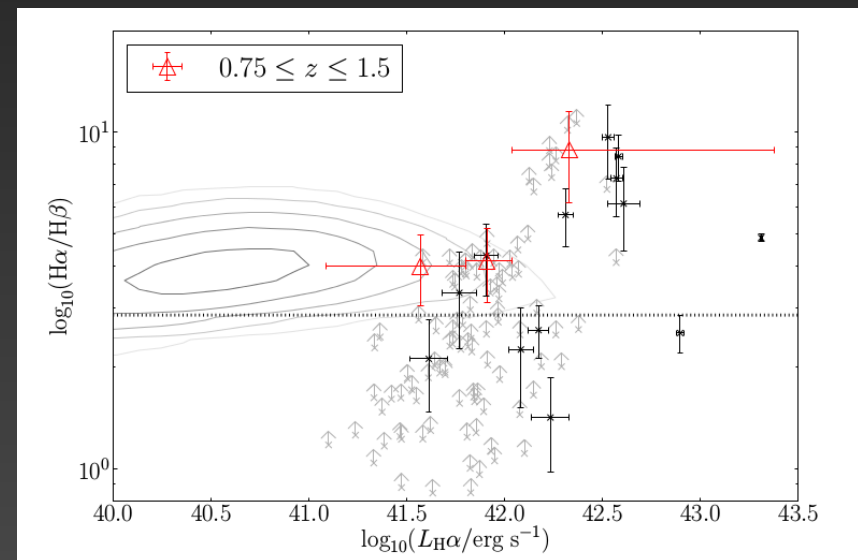
Galaxy spectra stacks at $0.75 \leq z \leq 1.5$

312 galaxies in 17 fields where both $H\alpha$ and $H\beta$ fall simultaneously in the WISP spectral coverage \rightarrow 128 galaxies after cleaning

Halpa Luminosities vs. Stellar Masses

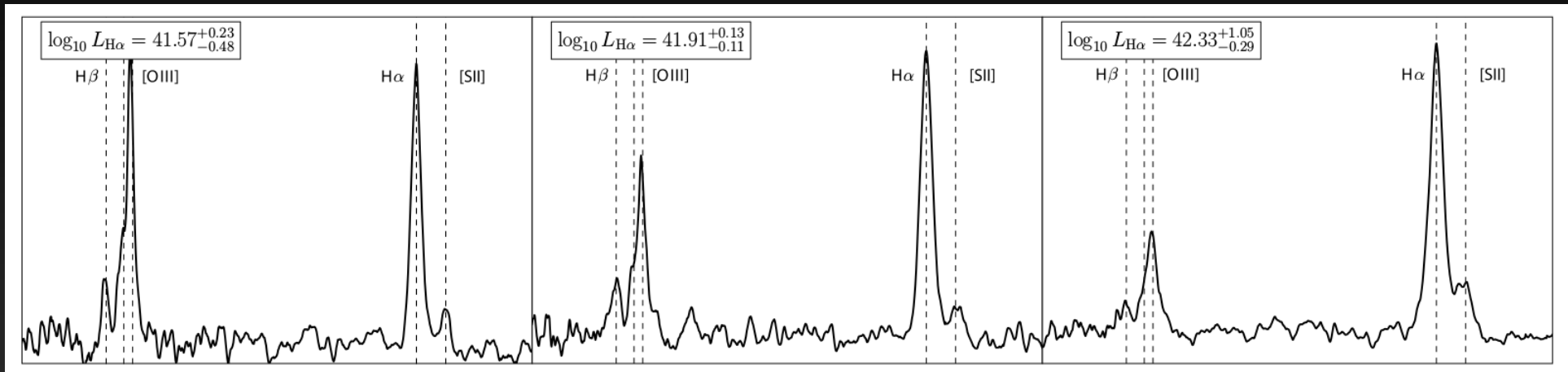


Balmer decrement vs. Halpa Luminosities



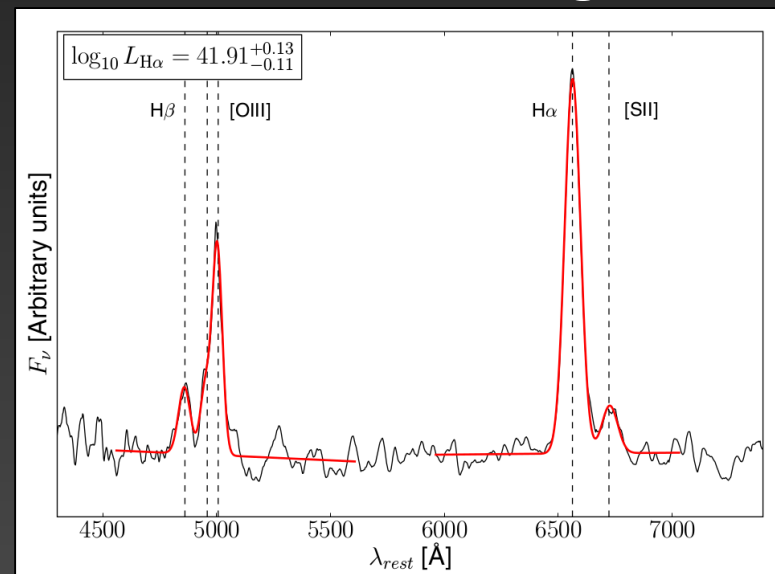
Galaxy spectra stacks at $0.75 \leq z \leq 1.5$

312 galaxies in 17 fields where both $H\alpha$ and $H\beta$ fall simultaneously in the WISP spectral coverage \rightarrow 128 galaxies after cleaning



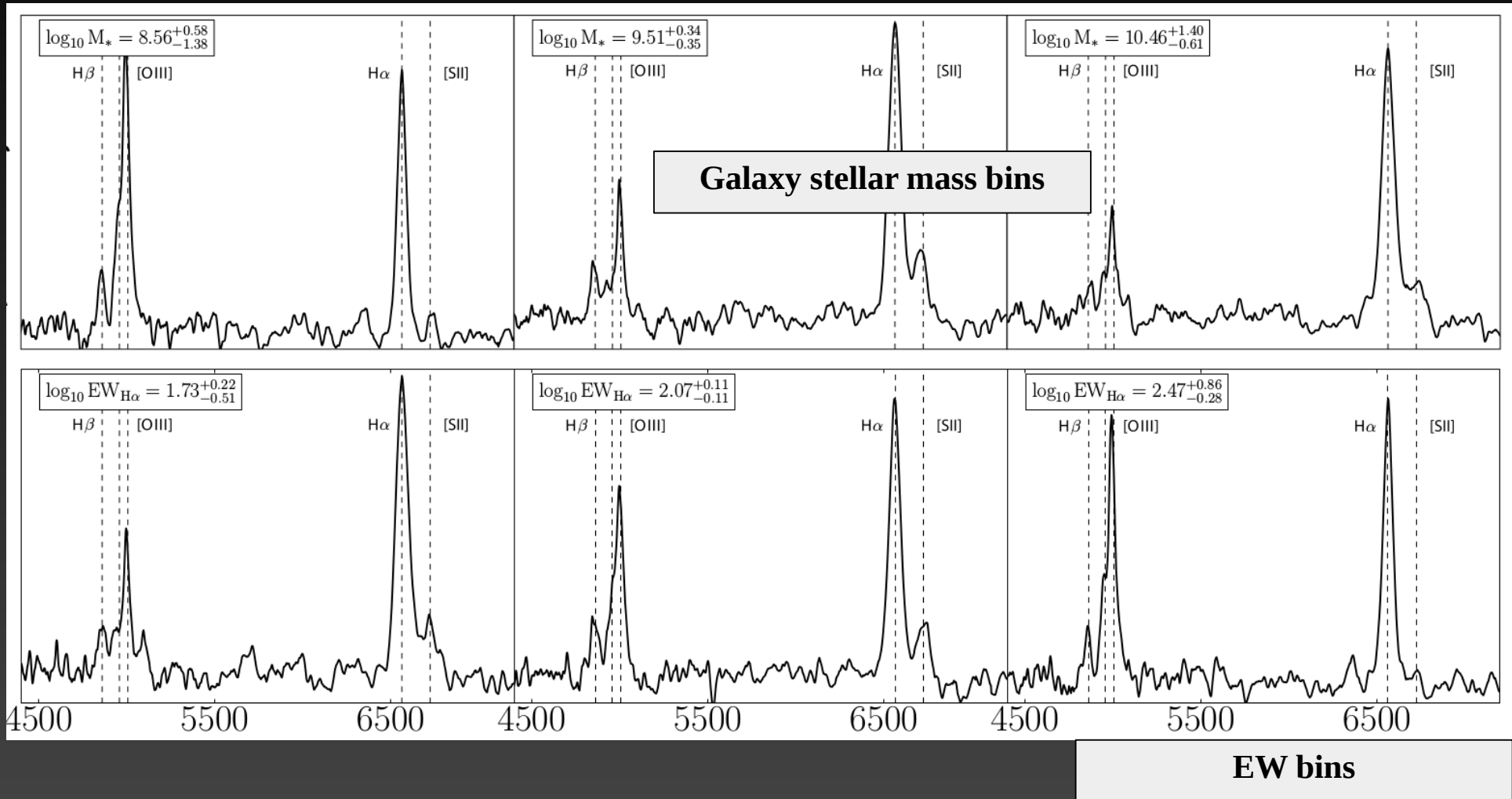
Luminosity bins

Rest-frame wavelength [\AA]



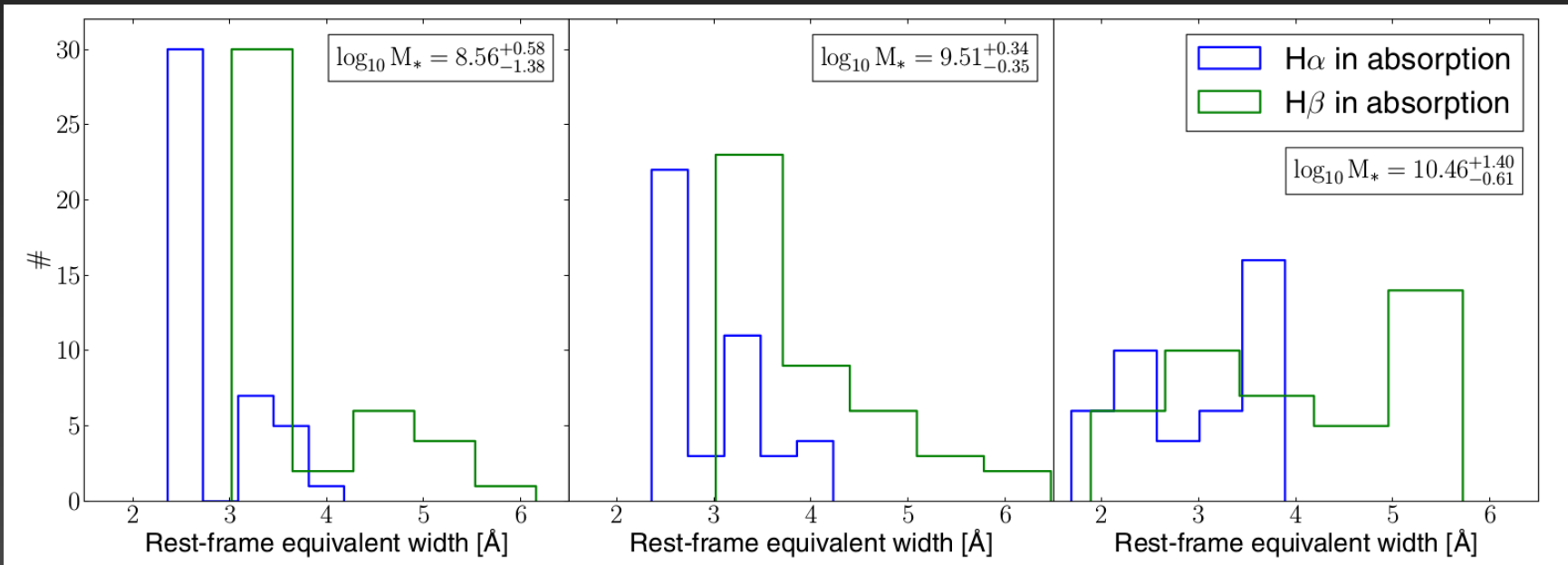
Galaxy spectra stacks at $0.75 \leq z \leq 1.5$

312 galaxies in 17 fields where both $H\alpha$ and $H\beta$ fall simultaneously in the WISP spectral coverage \rightarrow 128 galaxies after cleaning



Emission-line contamination

- H α and H β absorption ($\sim 25\%$ in H β); BC03 models



Emission-line contamination

- H α and H β absorption ($\sim 25\%$ in H β); BC03 models
- [N II] ($\sim 15\%$ in the worst case); Erb et al. 2006

TABLE 2
OXYGEN ABUNDANCES AND GAS FRACTIONS

Bin	Stellar Mass ^a ($10^{10} M_{\odot}$)	$F_{H\alpha}$ ^b (10^{-17} ergs s $^{-1}$ cm $^{-2}$)	$F_{[N II]}$ ^b (10^{-17} ergs s $^{-1}$ cm $^{-2}$)	N2 ^c	12 + log (O/H) ^d	M_{bar} ^e ($10^{10} M_{\odot}$)	μ_{gas} ^f	y_{eff} ^g
1.....	0.27 \pm 0.15	20.5 \pm 0.5	<1.2	<-1.22	<8.20	2.7 \pm 1.7	0.85 \pm 0.12	<0.027
2.....	0.71 \pm 0.17	13.9 \pm 0.3	1.4 \pm 0.2	-1.00 ^{+0.07} _{-0.09}	8.33 ^{+0.07} _{-0.07}	2.1 \pm 0.6	0.63 \pm 0.12	0.013 \pm 0.003
3.....	1.5 \pm 0.3	18.7 \pm 0.4	2.7 \pm 0.3	-0.85 ^{+0.05} _{-0.06}	8.42 ^{+0.06} _{-0.05}	3.2 \pm 1.1	0.48 \pm 0.19	0.010 \pm 0.002
4.....	2.6 \pm 0.4	15.9 \pm 0.4	2.6 \pm 0.3	-0.78 ^{+0.05} _{-0.05}	8.46 ^{+0.06} _{-0.05}	4.0 \pm 0.9	0.33 \pm 0.12	0.007 \pm 0.001
5.....	4.1 \pm 0.6	24.3 \pm 0.5	5.3 \pm 0.4	-0.66 ^{+0.03} _{-0.04}	8.52 ^{+0.06} _{-0.05}	6.6 \pm 1.1	0.36 \pm 0.10	0.009 \pm 0.002
6.....	10.5 \pm 5.4	27.0 \pm 0.4	7.4 \pm 0.3	-0.56 ^{+0.02} _{-0.02}	8.58 ^{+0.06} _{-0.04}	13.1 \pm 5.6	0.22 \pm 0.11	0.007 \pm 0.001

^a Mean and standard deviation of stellar mass from SED fitting; we use a Chabrier (2003) IMF.

^b Fluxes of H α and [N II] λ 6584 from the composite spectra.

^c N2 \equiv log ($F_{[N II]}/F_{H\alpha}$).

^d Oxygen abundance from N2, using the calibration of Pettini & Pagel (2004).

^e Mean and standard deviation of the baryonic mass $M_{\text{gas}} + M_{\star}$, with gas masses determined from the Schmidt law as described in the text.

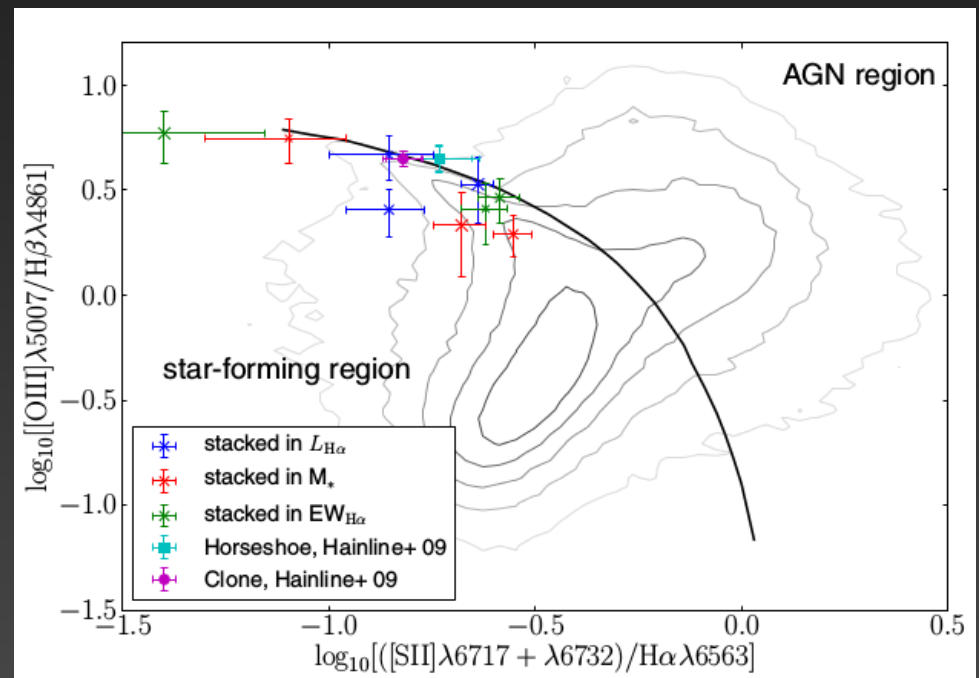
^f Mean and standard deviation of the gas fraction $\mu = M_{\text{gas}}/(M_{\text{gas}} + M_{\star})$.

^g Effective yield $y_{\text{eff}} = Z/\ln(1/\mu)$.

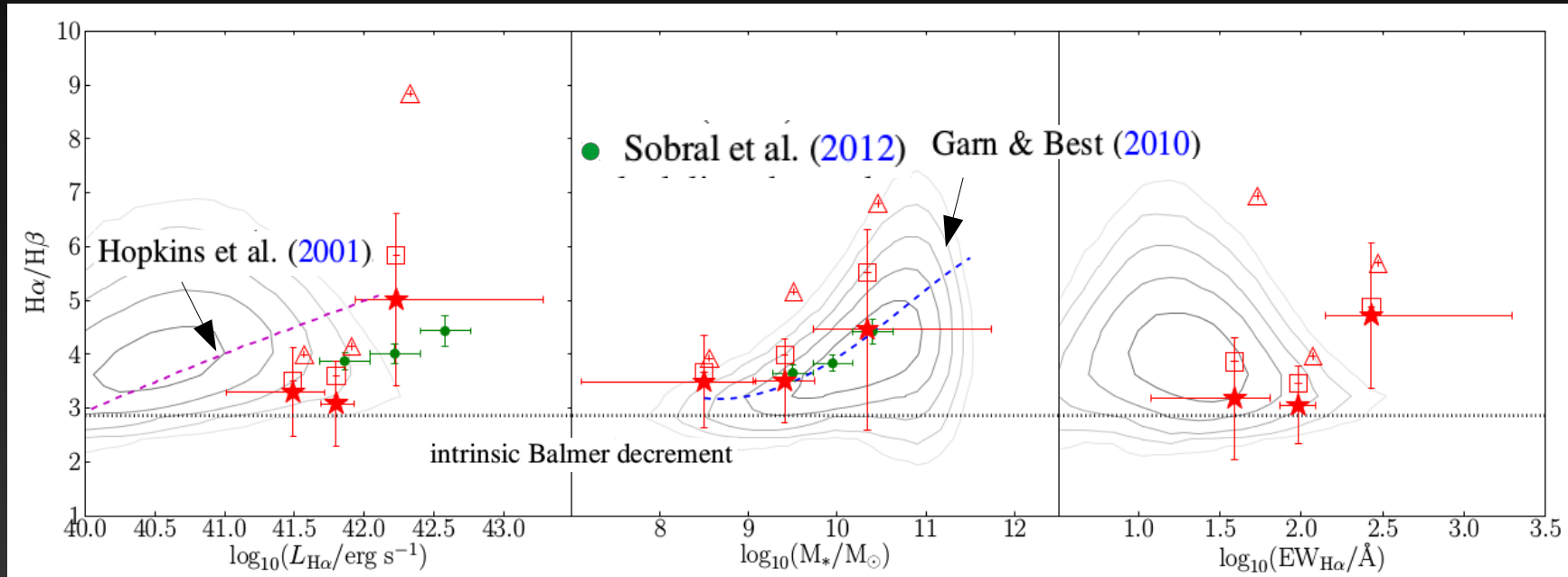
Emission-line contamination

- H α and H β absorption ($\sim 25\%$ in H β); BC03 models
- [N II] ($\sim 15\%$ in the worst case); Erb et al. 2006
- AGNs; BPT diagram

BPT diagram



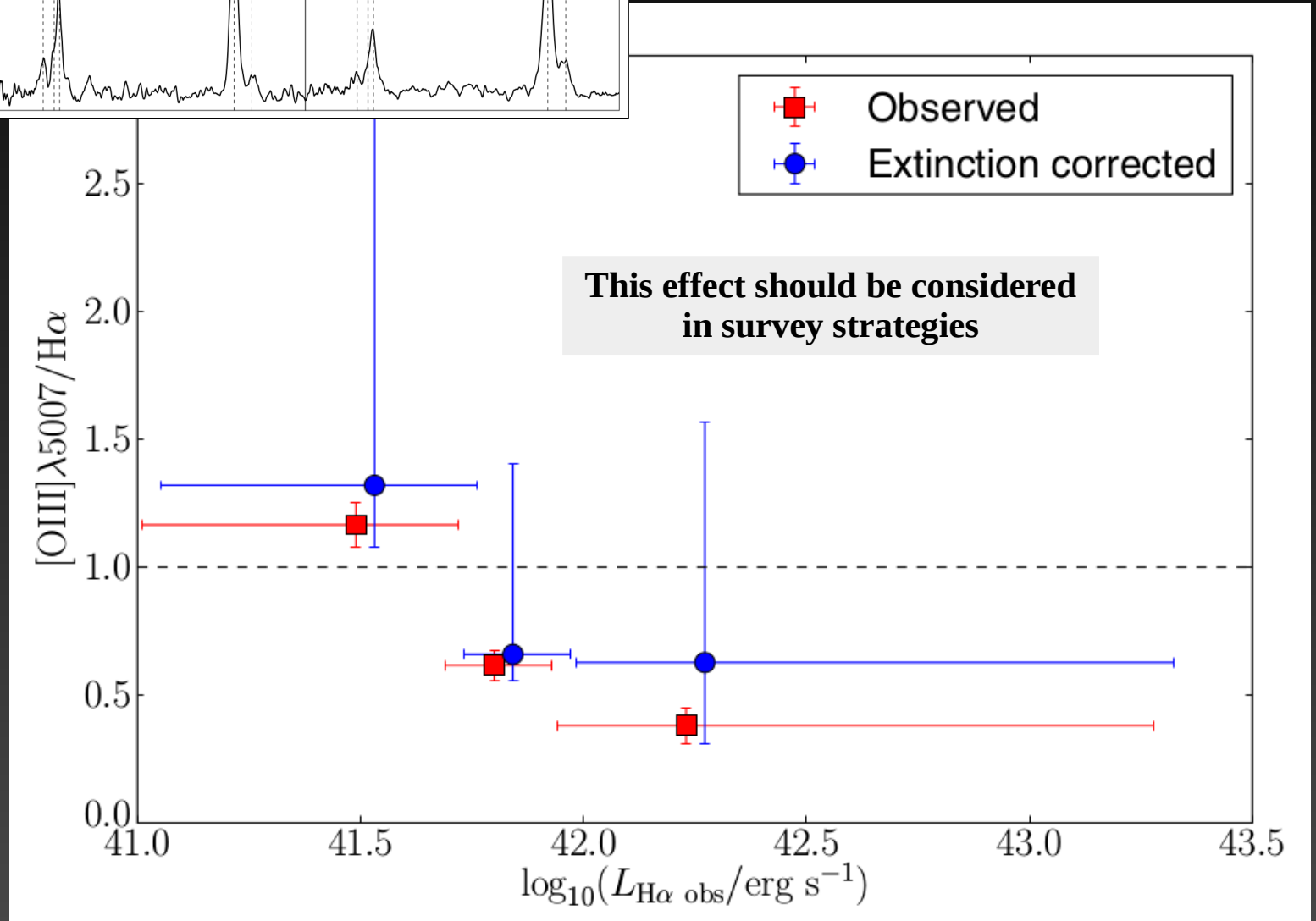
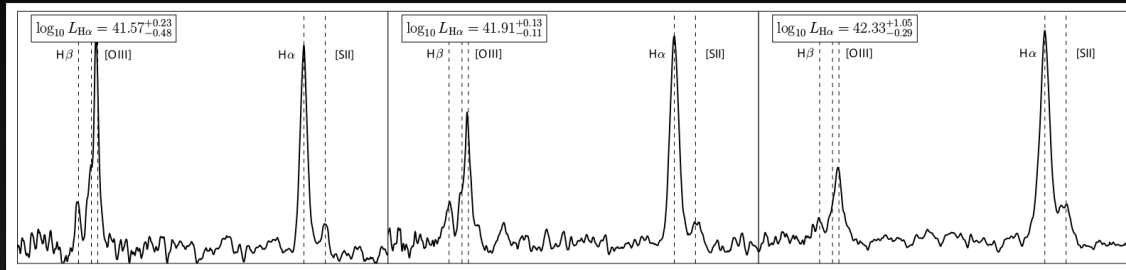
Balmer decrements at $z \sim 1$



**Balmer decrement versus H α luminosity,
galaxy stellar mass, and H α EW**

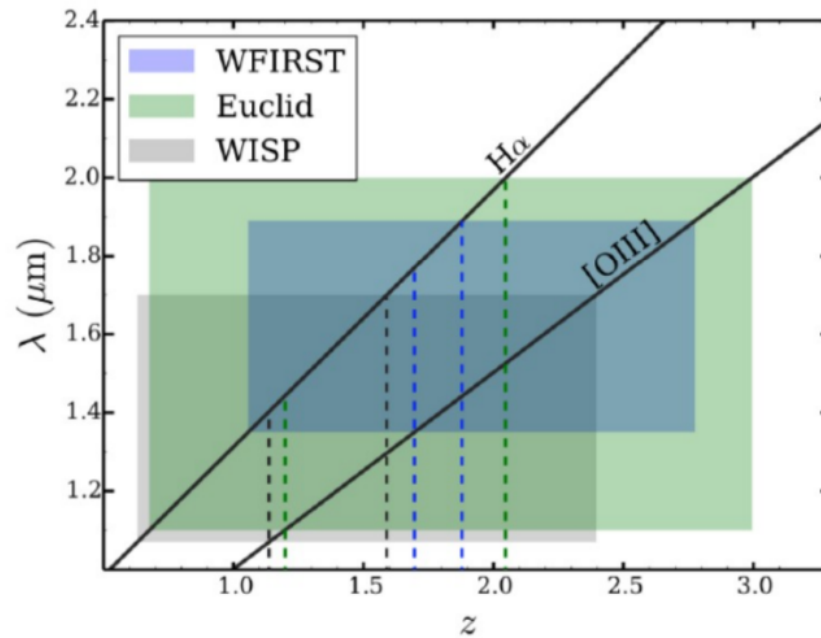
Important Conclusion: Typical assumption of assuming constant extinction for all luminosity overestimate the extinction for faint galaxies.

[OIII]/Halpha ratios

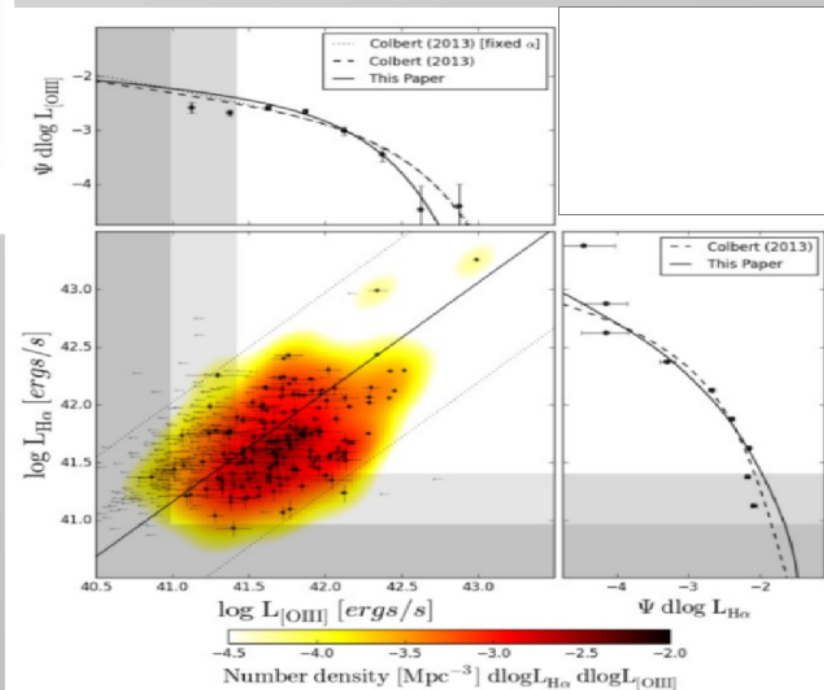


The future of near-IR surveys from space

Guiding Future IR Grism Surveys



WISP sample significantly increasing with time but also Euclid, WFIRST, DESI, eBOSS, 4MOST, ...

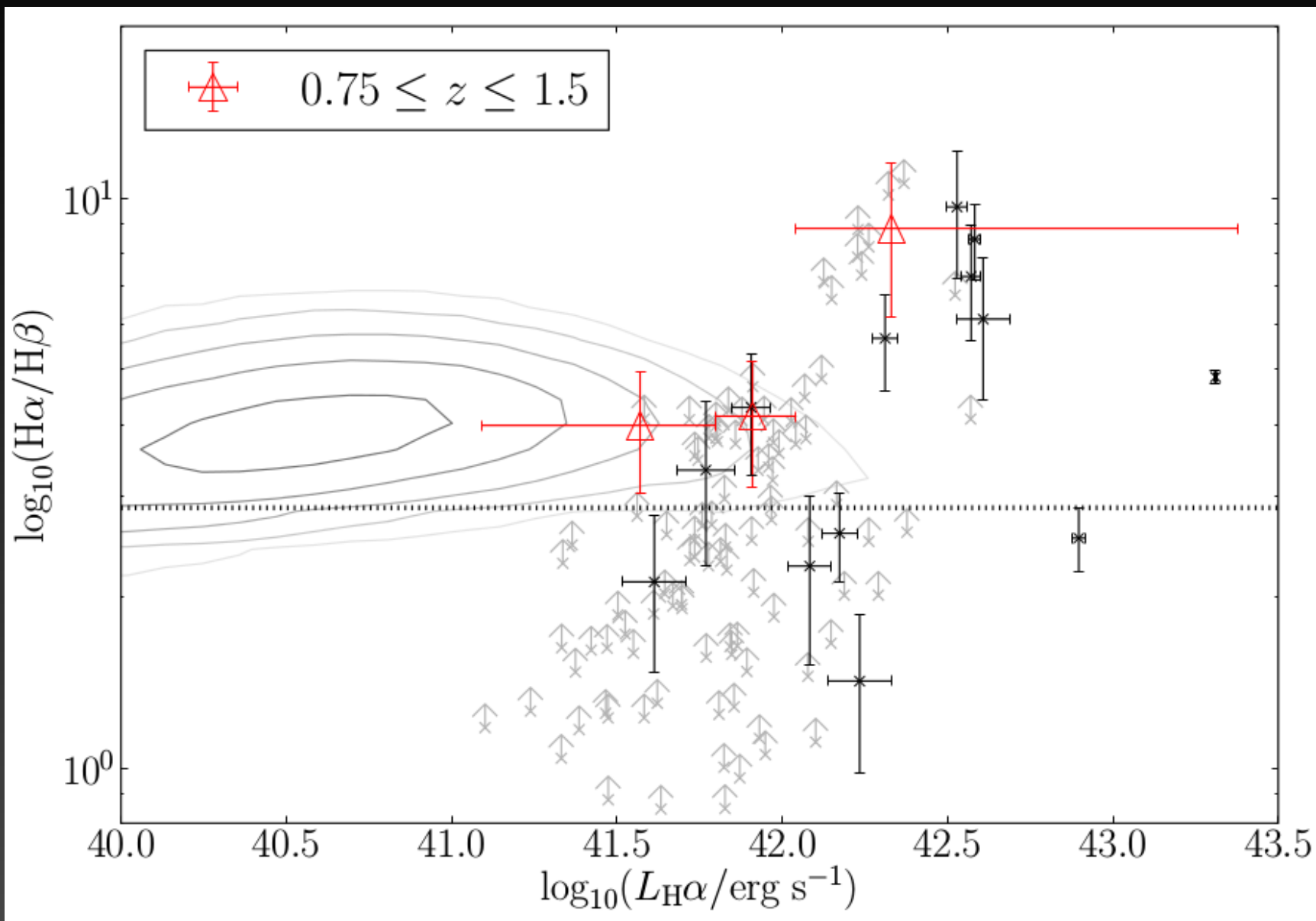


Mehta et al. (2015)

Summary and Conclusions

- 1.- The Balmer decrement is correlated with observed H α luminosity and galaxy stellar mass at $z \sim 1$. The faintest galaxies are consistent with no dust extinction.
- 2.- Clear evolution of dust extinction where for a given observed H α luminosity, galaxies are significantly less extinguished at higher redshifts. No evolution is found with galaxy stellar mass.
- 3.- The typical procedure of assuming a constant extinction for all luminosity significantly overestimate extinction for the lower luminosity galaxies.
- 4.- The H α /[O III] ratio is dependent on observed H α luminosity.
- 5.- WISP will improve these measurements in the near future.
- 6.- EUCLID and WFIRST will improve these measurements in the longer term future.

Backup



Backup

Table 1
Emission-line Ratios of Stacked Spectra in $0.75 \leq z \leq 1.5$

$\langle \log_{10} X \rangle$	$([\text{S II}] \lambda 6717 + \lambda 6732)/\text{H}\alpha \lambda 6563$	$[\text{O III}] \lambda 5007/\text{H}\beta \lambda 4861$
Stacks binned in $\text{H}\alpha$ luminosity, $X = L_{\text{H}\alpha}/\text{erg s}^{-1}$		
$41.57^{+0.48}_{-0.23}$	0.14 ± 0.04	4.65 ± 1.10
$41.91^{+0.11}_{-0.13}$	0.14 ± 0.03	2.55 ± 0.66
$42.33^{+0.29}_{-1.05}$	0.23 ± 0.02	3.37 ± 1.18
Stacks binned in galaxy stellar mass, $X = M_*/M_\odot$		
$8.56^{+1.38}_{-0.58}$	0.08 ± 0.03	5.58 ± 1.32
$9.51^{+0.35}_{-0.34}$	0.28 ± 0.03	1.95 ± 0.44
$10.46^{+0.61}_{-1.40}$	0.21 ± 0.03	2.15 ± 0.92
Stacks binned in $\text{H}\alpha$ equivalent width, $X = \text{EW}_{\text{H}\alpha}/\text{\AA}$		
$1.73^{+0.51}_{-0.22}$	0.24 ± 0.03	2.58 ± 0.84
$2.07^{+0.11}_{-0.11}$	0.26 ± 0.03	2.91 ± 0.69
$2.47^{+0.28}_{-0.86}$	0.04 ± 0.03	5.89 ± 1.63

Note. These are the values for plotting the BPT diagram shown in Figure 6.

Backup

Table 2
Dust Properties for WISP Galaxies

N^a	$\langle \log_{10}(X) \rangle$	H_α/H_β^b	H_α/H_β^c	H_α/H_β^d	$E(B - V)^e$ (mag)	$A_{H\alpha}^e$ (mag)	A_V^e (mag)
Galaxy spectra stacked in $H\alpha$ luminosity, $X \equiv L_{H\alpha}/\text{erg s}^{-1}$							
43	$41.57^{+0.23}_{-0.48}$	3.99 ± 0.95	3.51 ± 0.85	3.29 ± 0.82	0.12 ± 0.21	0.40 ± 0.71	0.48 ± 0.86
43	$41.91^{+0.13}_{-0.11}$	4.14 ± 1.03	3.59 ± 0.91	3.08 ± 0.79	0.06 ± 0.22	0.21 ± 0.73	0.25 ± 0.89
42	$42.33^{+1.05}_{-0.29}$	8.84 ± 2.66	5.84 ± 1.86	5.01 ± 1.60	0.48 ± 0.27	1.59 ± 0.98	1.94 ± 1.17
Galaxy spectra stacked in stellar mass, $X \equiv M_*/M_\odot$							
43	$8.56^{+0.58}_{-1.38}$	3.92 ± 0.93	3.66 ± 0.87	3.49 ± 0.85	0.17 ± 0.21	0.57 ± 0.71	0.69 ± 0.85
43	$9.51^{+0.34}_{-0.35}$	5.16 ± 1.10	3.99 ± 0.88	3.50 ± 0.78	0.17 ± 0.19	0.57 ± 0.65	0.70 ± 0.78
42	$10.46^{+1.40}_{-0.61}$	6.80 ± 2.79	5.52 ± 2.29	4.46 ± 1.86	0.38 ± 0.36	1.26 ± 1.22	1.54 ± 1.47
Galaxy spectra stacked in rest-frame $H\alpha$ equivalent width, $X \equiv \text{EW}_{H\alpha}/\text{\AA}$							
43	$1.73^{+0.22}_{-0.51}$	6.93 ± 2.16	3.86 ± 1.36	3.18 ± 1.13	0.09 ± 0.30	0.30 ± 1.01	0.36 ± 1.23
43	$2.07^{+0.11}_{-0.11}$	3.96 ± 0.90	3.46 ± 0.80	3.05 ± 0.72	0.06 ± 0.20	0.19 ± 0.67	0.23 ± 0.81
42	$2.47^{+0.86}_{-0.28}$	5.69 ± 1.58	4.88 ± 1.37	4.72 ± 1.35	0.43 ± 0.24	1.42 ± 0.88	1.73 ± 1.05

Notes. All observables are given for nebular properties.

^a N is the number of stacked galaxy spectra in the bin.

^b No correction applied.

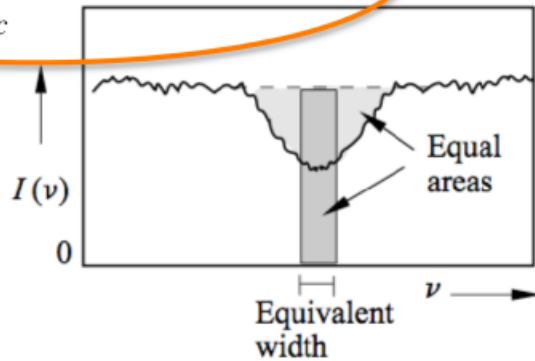
^c Corrected only for $H\alpha$ and $H\beta$ absorption lines (see Section 2.6).

^d Corrected for $H\alpha$ and $H\beta$ absorption lines and $[\text{N II}]$ contamination (see Section 2.6).

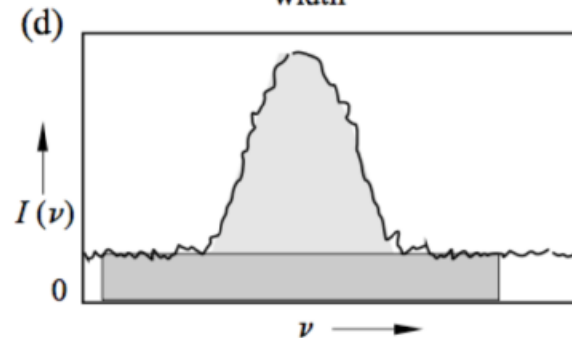
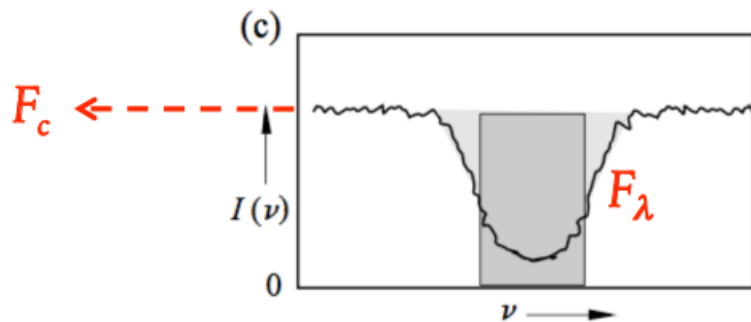
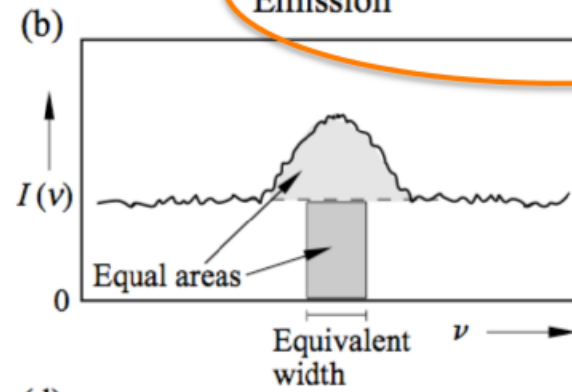
^e Calculated from the absorption line and $[\text{N II}]$ corrected Balmer decrements.

The Equivalent width concept

$$EW = \int_{\lambda_1}^{\lambda_2} \frac{F_c - F_\lambda}{F_c} d\lambda \quad \text{Absorption}$$

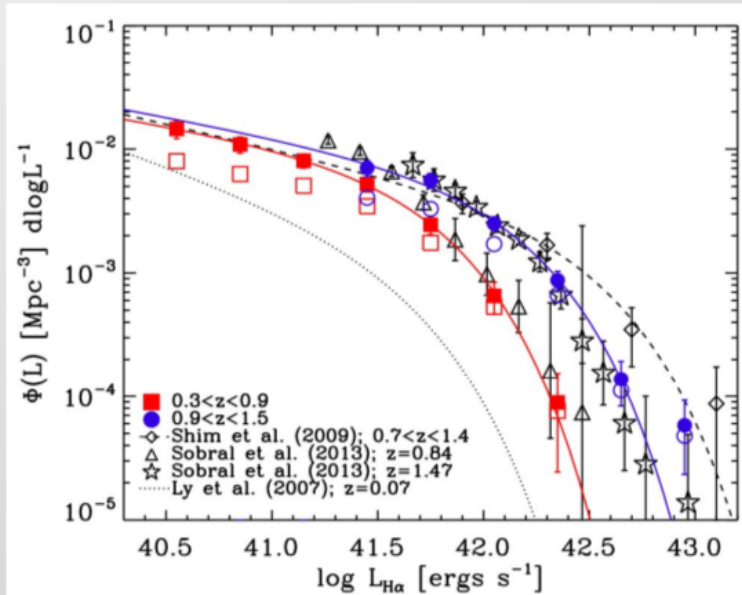


$$\text{Emission} \quad EW = \int_{\lambda_1}^{\lambda_2} \frac{F_\lambda - F_c}{F_c} d\lambda$$

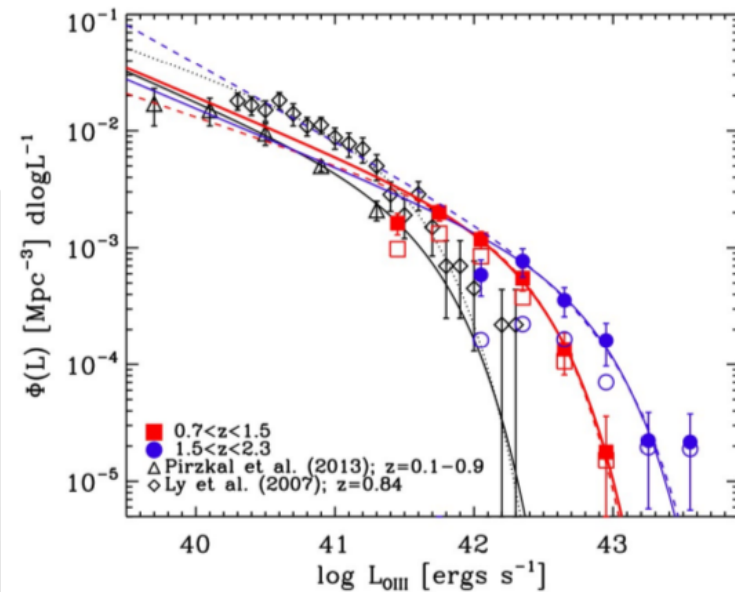


Other WISP science topics (1/3)

Galaxy Luminosity Functions

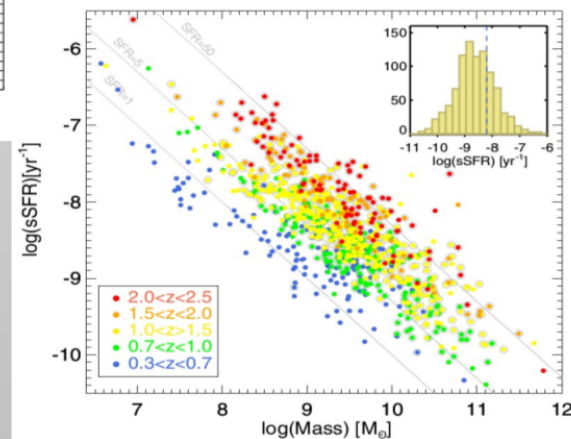
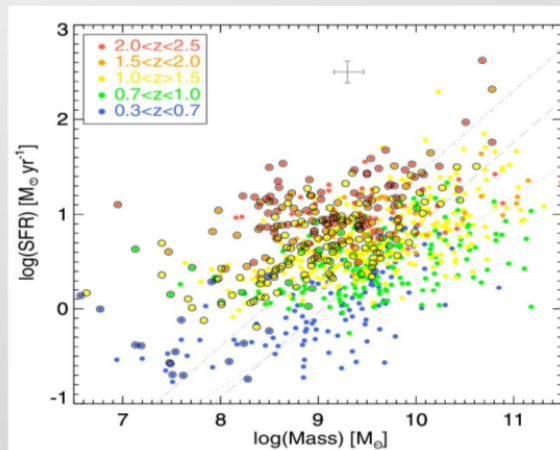


Colbert et al. (2013)



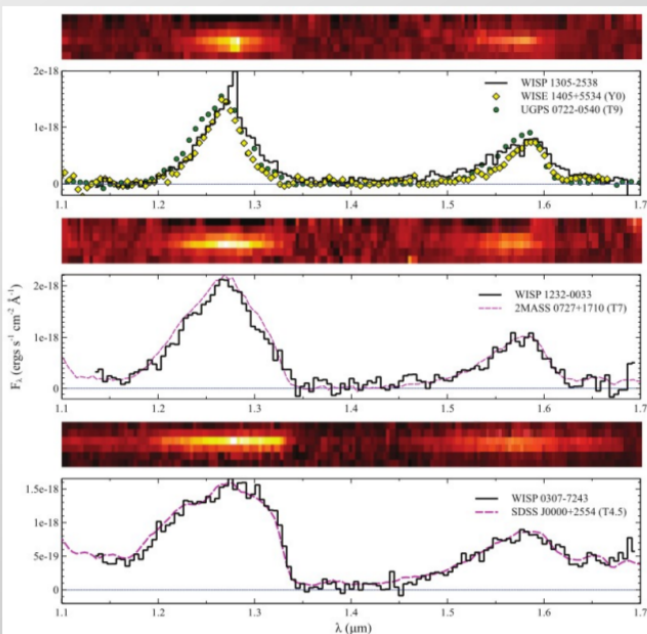
Other WISP science topics (2/3)

The Star-forming Main Sequence



Atek et al. (2014)

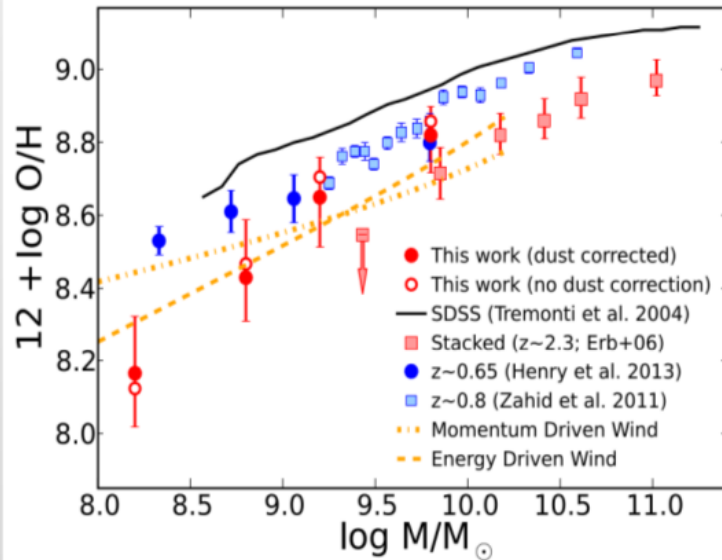
Discovery of Three Distant Cold Brown Dwarfs



Masters et al. (2012)

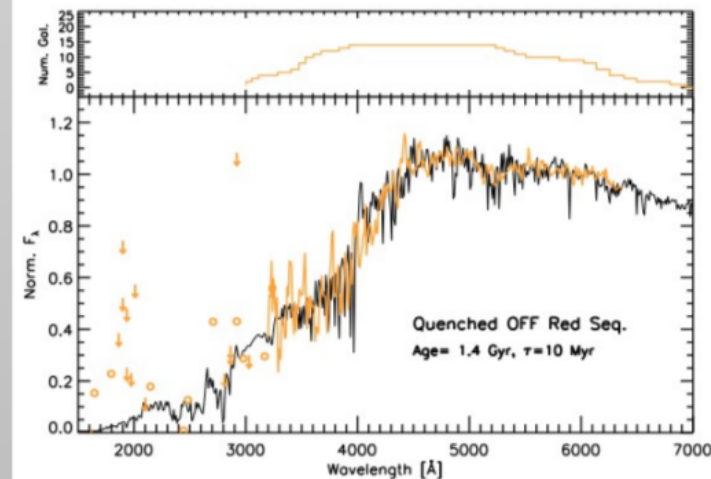
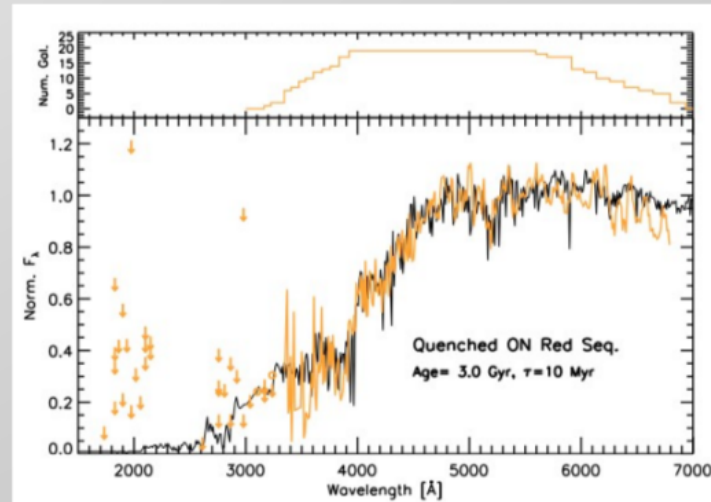
Other WISP science topics (3/3)

Mass-metallicity & Early-type Galaxies



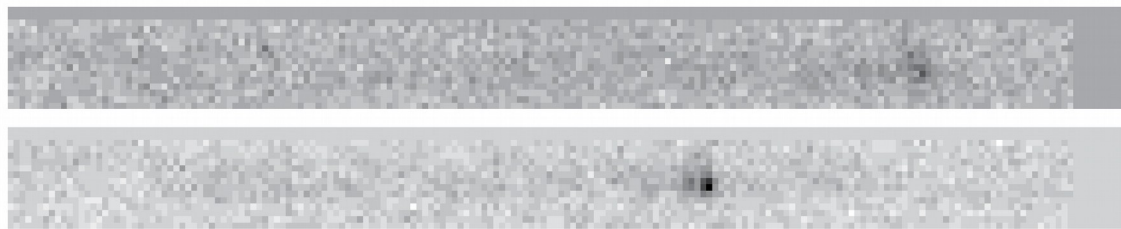
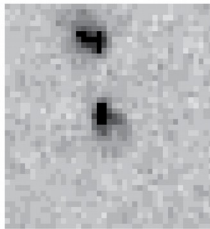
Henry et al. (2013)

Bedregal et al. (2013)



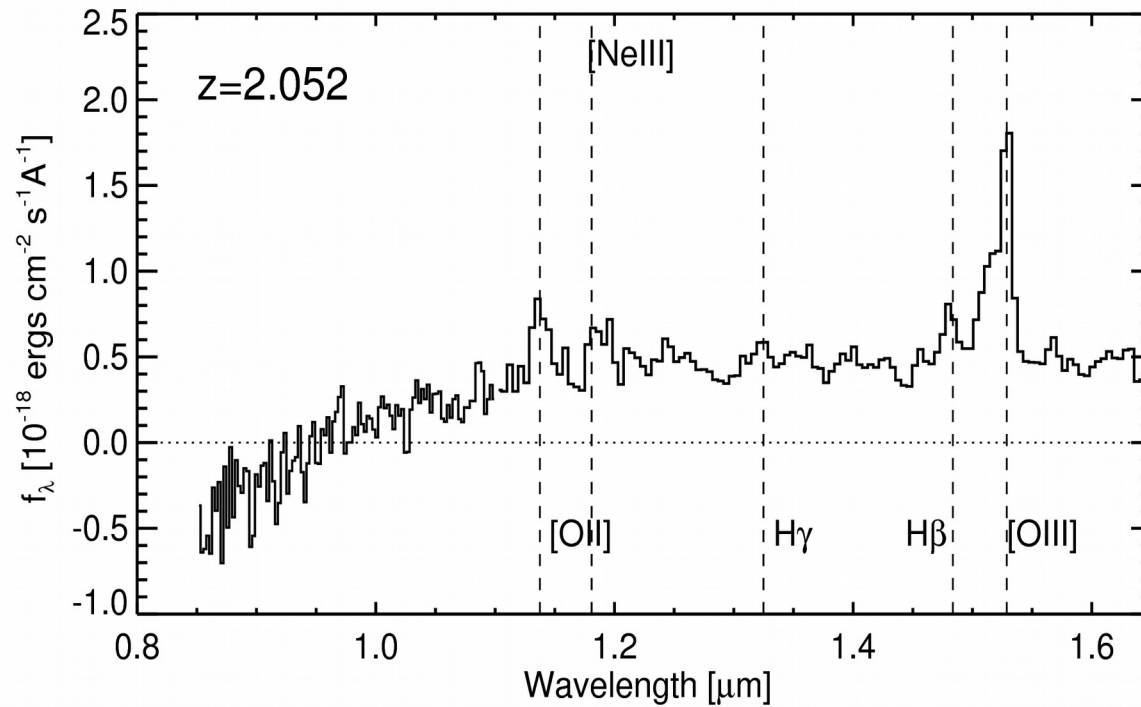
The WISP survey

F110W



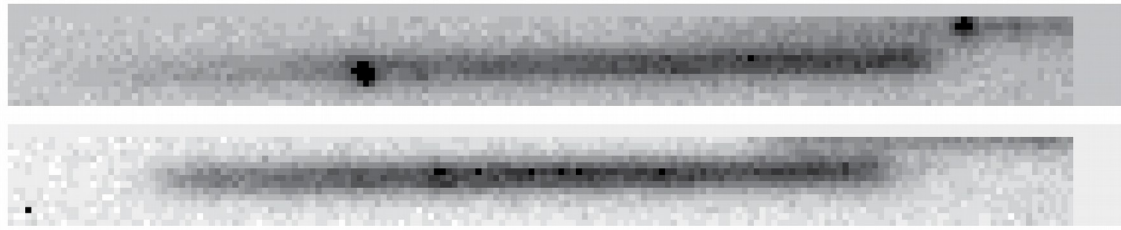
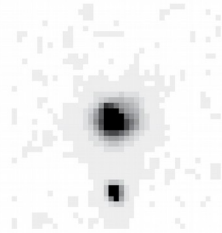
G102

G141



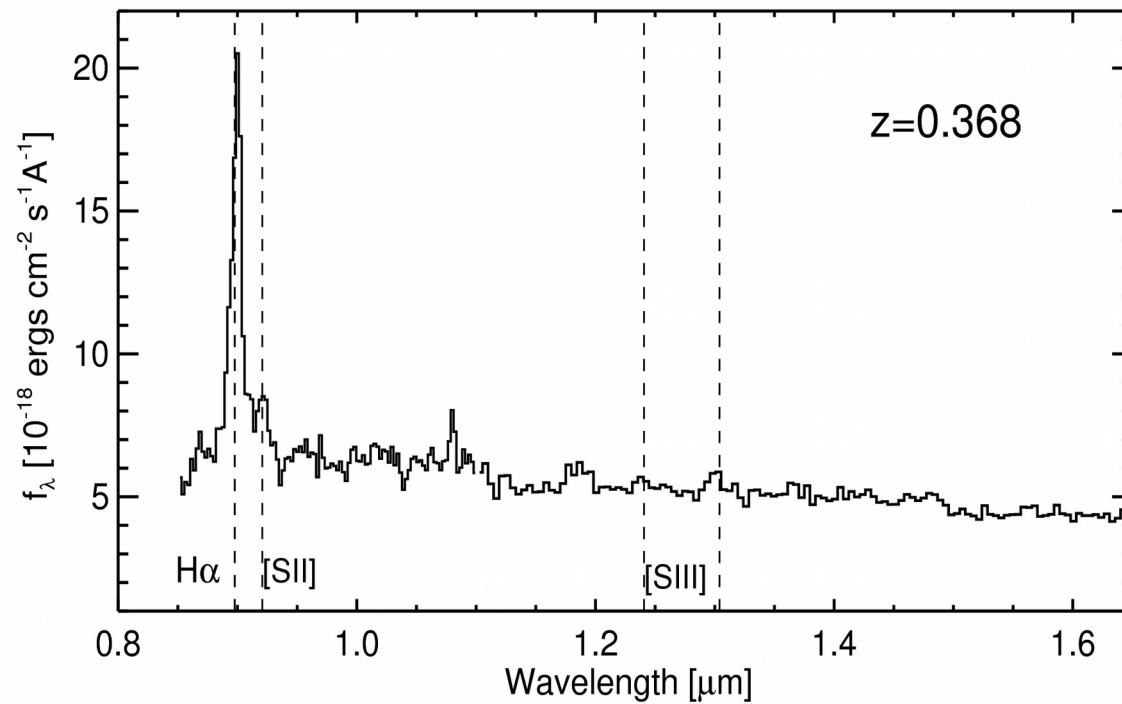
The WISP survey

F110W



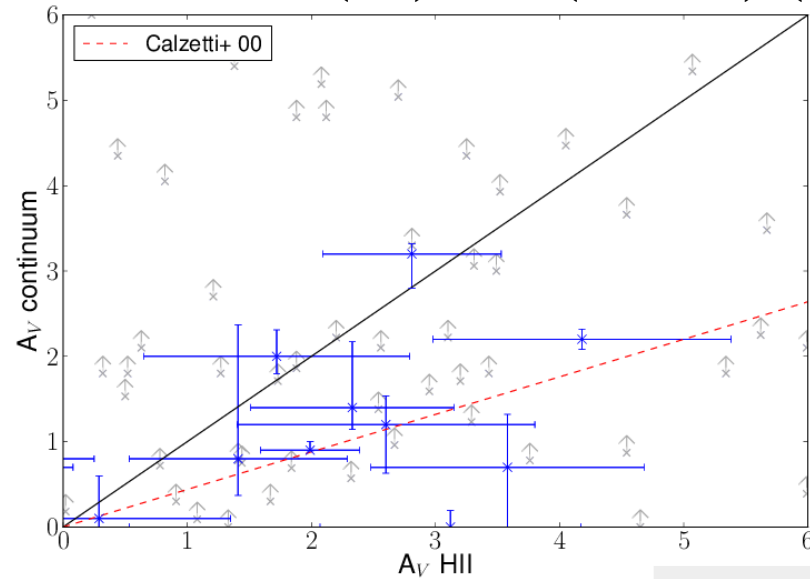
G102

G141



Stellar vs. nebular extinction

Calzetti et al. 2000; $E(B-V)_{\text{stellar}} = (0.44 \pm 0.03) E(B-V)$



Stellar extinction versus
nebular extinction